Purification of active human vacuolar H+-ATPase in native lipid-containing nanodiscs

Rebecca A. Oot[1], Yeqi Yao[2], Morris F. Manolson[2], and Stephan Wilkens[1],*
From the [1]Department of Biochemistry and Molecular Biology, SUNY Upstate Medical University, Syracuse, New York, USA; [2]Faculty of Dentistry, University of Toronto, Toronto, Ontario, Canada

Edited by Karen Fleming

Vacuolar H+-ATPases (V-ATPases) are large, multisubunit proton pumps that acidify the lumen of organelles in virtually every eukaryotic cell and in specialized acid-secreting animal cells, the enzyme pumps protons into the extracellular space. In higher organisms, most of the subunits are expressed as multiple isoforms, with some enriched in specific compartments or tissues and others expressed ubiquitously. In mammals, subunit *a* is expressed as four isoforms (*a*1-4) that target the enzyme to distinct biological membranes. Mutations in *a* isoforms are known to give rise to tissue-specific disease, and some *a* isoforms are upregulated and mislocalized to the plasma membrane in invasive cancers. However, isoform complexity and low abundance greatly complicate purification of active human V-ATPase, a prerequisite for developing isoform-specific therapeutics. Here, we report the purification of an active human V-ATPase in native lipid nanodiscs from a cell line stably expressing affinity-tagged *a* isoform 4 (*a*4). We find that exogenous expression of this single subunit in HEK293F cells permits assembly of a functional V-ATPase by incorporation of endogenous subunits. The ATPase activity of the preparation is >95% sensitive to concanamycin A, indicating that the lipid nanodisc-reconstituted enzyme is functionally coupled. Moreover, this strategy permits purification of the enzyme's isolated membrane subcomplex together with biosynthetic assembly factors coiled-coil domain–containing protein 115, transmembrane protein 199, and vacuolar H+-ATPase assembly integral membrane protein 21. Our work thus lays the groundwork for biochemical characterization of active human V-ATPase in an *a* subunit isoform-specific manner and establishes a platform for the study of the assembly and regulation of the human holoenzyme.

The internal pH of subcellular compartments, critical to their identity and function, is maintained by a large multisubunit ATP hydrolysis–driven proton pump referred to as vacuolar H+-ATPase (V-ATPase). V-ATPase activity is essential for diverse cellular processes including pH and ion homeostasis, endocytosis and exocytosis, protein degradation, zymogen activation, insulin secretion, neurotransmitter release, and pro-growth and developmental signaling pathways including Wnt, Notch, and mTOR (1, 2). The V-ATPase can also be found on the plasma membrane of dedicated acid-secreting cells such as osteoclasts and renal α-intercalated cells where the enzyme is required for bone demineralization and urinary acidification, respectively (3, 4). Aberrant V-ATPase activity is associated with numerous diseases including renal tubular acidosis (5), osteopetrosis (6), neurodegeneration (7, 8), glycosylation disorders (9), and cancer (10). V-ATPase function is also important in both pathogen invasion and host protection, with several pathogenic bacteria found to secrete V-ATPase-specific virulence factors to escape host degradative pathways (11–13). Furthermore, an increasing number of studies have implicated V-ATPase as being essential for efficient infection by viruses including HIV, influenza, Zika, Dengue, and Ebola, and more recently, the enzyme was identified as being part of the SARS-CoV-2 interactome (14–18).

The V-ATPase is composed of a cytosolic ATPase subcomplex, called V_1, and a membrane integral proton channel, termed V_o (Fig. 1A). V_1 is composed of eight subunits, A-H, with a stoichiometry of $A_3B_3CDE_3FG_3H$, and V_o contains six subunits, *a*, *c*, *c*", *d*, *e*, and *f*, in the ratio $ac_9c"def$ (19). In mammals, two additional polypeptides called Ac45 or S1 (gene name ATP6AP1) and prorenin receptor (PRR; gene name ATP6AP2) are anchored at the luminal (or extracellular) side of the V_o *via* their C-terminal transmembrane α helices (20–24). V-ATPase is a rotary motor enzyme: cyclic ATP hydrolysis at three catalytic sites in the catalytic hexamer (A_3B_3) drives rotation of subunits D, F, *d*, and the membrane integral ring of ten *c* subunits (c_9c"; *c*-ring) (Fig. 1A). During rotation, lipid-exposed glutamic acid residues on the *c* (and *c*") subunits transfer protons between cytosolic and luminal aqueous half channels located in the membrane integral C-terminal domain of subunit *a* (25). Subunit *a*'s cytosolic N-terminal domain forms a hub for interactions with cytoplasmic subunits (C, H, and three EG heterodimers), and together, these interactions hold the catalytic hexamer static to permit productive rotary catalysis. As a dynamic multisubunit molecular machine, enzyme function requires the concerted action of all ~30 polypeptides in the complex.

V-ATPase activity is regulated *in vivo* by a unique mechanism termed "reversible disassembly", characterized by a dramatic (and reversible) structural rearrangement wherein V_1 is

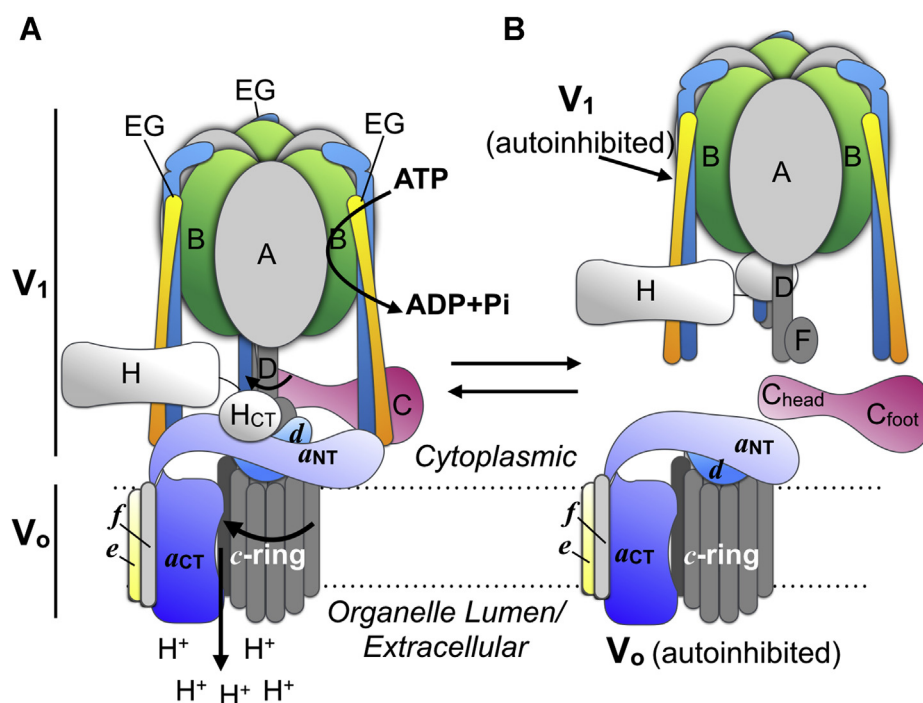* For correspondence: Stephan Wilkens, wilkenss@upstate.edu.

Figure 1. Subunit architecture and regulation of the human V-ATPase. *A*, schematic of the V-ATPase subunit architecture. Subunits belonging to the cytosolic V_1-ATPase subcomplex are designated in capital letters (A-H) and those that are part of the integral V_o proton channel subcomplex in lower case italics (*a*, *d*, *e*, *f* and *c*-ring). The single copy, ~100-kDa subunit *a* is shown in *blue* with the C-terminal integral (a_{CT}) and cytosolic N-terminal (a_{NT}) domains labeled. For clarity, Ac45 (or S1) and prorenin receptor are not shown. *B*, regulation of V-ATPase activity by reversible disassembly. V-ATPase, vacuolar H^+-ATPase.

released into the cytosol, leaving behind free V_o in the membrane (1, 26) (Fig. 1B). Upon disassembly, both subcomplexes become autoinhibited in that V_1 no longer hydrolyzes MgATP and V_o does not catalyze passive proton transport (27–30). Reversible disassembly has been well characterized in yeast (31, 32) and insects (33, 34), but the process has also been observed in cultured mouse dendritic cells (35, 36), hippocampal neurons (37), rat hepatocytes (38), and established mammalian (39, 40) and human cell lines (15, 41–43).

A fascinating, yet complicating, aspect in the study of V-ATPase is the presence of subunit isoforms (44, 45). In yeast, only subunit *a* is expressed as two isoforms, presenting an ideal system for study of different isoforms containing V-ATPases (46, 47). Although the two isoforms carry out the same function in the complexes that harbor them, the two enzyme subpopulations differ in subcellular localization, activity, and regulation (48–52), highlighting the importance of *a* isoforms in shaping unique properties of the enzyme. Furthermore, it has been shown in yeast that the cytosolic N-terminal domain of subunit *a* isoforms is responsible for targeting the enzyme to different biological membranes (48, 50). In higher organisms, most enzyme subunits are expressed as multiple isoforms or splice variants (44, 45), including V_1 subunits B, C, E, G, H, and V_o subunits *d*, *e*, and *a*. Notably, subunit *a* is expressed as four isoforms (*a*1–4) in mammals that, like in yeast, are targeted to different cellular membranes (45). V-ATPase is found on intracellular compartments and organelles in all eukaryotic cells, and ubiquitously expressed isoforms *a*1, *a*2, and *a*3 reside on such membranes (45). Isoform *a*1, while widely expressed, is highly enriched in the brain

where it is required for neurotransmitter loading into synaptic vesicles (53, 54). Isoform *a*2 has been observed in early endosomes and Golgi (55, 56) and *a*3 in lysosomes and secretory granules (57–59). Isoform *a*4 displays the narrowest range of tissue expression, found in the kidney, epididymis, inner ear, and olfactory cells (5, 60–62). In cell types that are specialized for acid secretion, V-ATPases containing either *a*3 or *a*4 are targeted to the plasma membrane (44). For example, isoform *a*3 is enriched in the plasma membrane of osteoclasts where enzyme function is required for bone resorption (6, 45). In renal α-intercalated cells, isoform *a*4 is enriched in the apical membrane where it acidifies the urine, which is critical to maintenance of systemic pH homeostasis (2, 5). It should be noted that while some tissues or cell types contain an enriched *a* subunit isoform population required for specialized function, such subpopulations coexist with V-ATPases containing different *a* isoforms found on other compartments in the same cell (63, 64). Furthermore, some isoforms of cytosolic V_1 subunits associate with V_o complexes containing specific *a* isoforms, forming unique complexes (Fig. S1) (37, 65, 66). While the isoform composition of some specialized complexes has been experimentally determined or postulated based on expression pattern, a comprehensive picture of the isoforms comprising each V-ATPase in a cell remains unclear. Moreover, it is unknown whether such V-ATPase subpopulations contain any intrinsic functional differences. Despite these layers of complexity, the importance of different *a* isoforms in specialized roles is exemplified by their mutation giving rise to tissue-specific diseases (5, 6, 67, 68). Furthermore, some *a* isoforms are upregulated and mislocalized to the plasma

membrane in invasive cancer cells (10, 69), and isoform knockdown or global enzyme inhibition decreases invasion, induces apoptosis, and increases drug sensitivity (10). However, total loss of enzyme function is embryonic lethal (70, 71), and currently available compounds are pan-V-ATPase inhibitors, making the design of isoform-specific therapeutics a priority.

The high level of V-ATPase expression in certain organs or tissues (*e.g.*, brain, kidney, insect midgut, and osteoclasts) has permitted purification of the animal enzyme in sufficient quantities for biochemical and biophysical experiments (72–77), with much foundational knowledge of the structure and function of V-ATPases coming from such studies. Recently, Wang *et al.* (23) presented high-resolution cryo-EM structures of a human V-ATPase purified from suspension HEK293 cells. While the structures provided a first detailed view of the human a1-containing enzyme, the use of a *Legionella pneumophila* virulence factor (SidK; (11)) for affinity capture rendered the enzyme inactive, precluding its use in biochemical studies requiring active enzyme.

The roles of V-ATPase in normal physiology and disease are well documented and continue to be studied in animal models, in case studies of human disease, and on a cellular level. *In vitro* studies of the human enzyme have been more limited, likely due in part to isoform complexity and a lack of a sustainable source of human enzyme for protein purification. Purified, active human V-ATPase of a defined *a* subunit isoform composition would allow analyses of possible intrinsic differences in biochemical properties of enzyme sub-populations, as seen for the yeast enzyme. Furthermore, such a system would greatly simplify characterization of V-ATPase-binding partners and potential regulators, permitting determination of how these interact with the enzyme, whether they are isoform specific, and if they directly impact V-ATPase assembly or function. Moreover, exploring the potential for isoform-specific activity modulation would benefit from *in vitro* biochemical analyses of purified, active enzyme with specific *a* subunit isoform content.

Here, we present purification of active human V-ATPase from suspension HEK293 cells stably transfected with affinity-tagged subunit isoform *a*4. Affinity-captured complexes in native lipid-containing nanodiscs were further purified *via* glycerol density centrifugation, permitting isolation of intact V-ATPase as well as free V_o subcomplex. The preparation has a specific ATPase activity of up to 5 μmol × (min × mg)$^{-1}$, which is sensitive to the V-ATPase-specific inhibitor concanamycin A (ConA). MS analysis showed that most subunit isoforms that were part of the purified *a*4-containing complex were of ubiquitous nature. Taken together, the here-developed procedure will allow purification and biochemical characterization of active human V-ATPase complexes with defined subunit *a* isoform content.

Results

So far, mammalian V-ATPase has either been purified from animal organ tissue using conventional biochemical

methods or, more recently, *via* affinity capture using the inhibitory virulence factor SidK (22, 23). As there is a need for purified active human V-ATPase of defined isoform composition and because human organ tissue is not widely available, we sought to develop a system for purification of the human enzyme in an *a* subunit isoform–specific fashion. Previously, transient transfection of adherent HEK293 cells with FLAG-tagged *a* isoforms was used to examine subunit glycosylation (78, 79). These studies also showed that the exogenously expressed *a* isoforms were properly post-translationally modified and assembled with endogenous subunits to form intact V-ATPase complexes (78). We used this plasmid for stable expression of C-terminally FLAG-tagged isoform *a*4 in suspension HEK293 (FreeStyle 293F) cells. This cell line was chosen solely for the purpose of accumulation of sufficient cell mass for purification of the low-abundance V-ATPase and not based on possible endogenous isoform content (evidence suggests that while HEK cells are derived from fetal kidney tissue, the origin of this cell line is most likely adrenal (80, 81)). We find that expression of this single, affinity-tagged, ~100-kDa *a*4 subunit permits both assembly of intact V-ATPase (by incorporation of endogenous subunits) and affinity purification of the resulting ~1-MDa multisubunit complex. In our hands, initial preparations of the enzyme purified in detergent displayed very little activity (Fig. S2), in accord with early biochemical purifications of the animal enzyme that reported a lipid requirement for activity (73, 82, 83). Lipid nanodiscs, synthetic lipid bilayers stabilized by binding membrane scaffold protein (MSP) (84), have been widely used for structural and biochemical analysis of membrane proteins. Previously, our laboratory has found that reconstitution of yeast V-ATPase into native lipid-containing nanodiscs yielded robust specific activity and superior stability of the complex (85). Here, a similar procedure was used for purification of the human enzyme, wherein a dense membrane/organelle containing fraction was solubilized in dodecyl maltoside in presence of MSP, followed by slow detergent removal, and spontaneous formation of lipid nanodiscs. Nanodisc-reconstituted total membrane proteins were then applied to a FLAG column for affinity capture of the *a*4-containing V-ATPase (Fig. 2*A*). As the V-ATPase is regulated *in vivo* by reversible disassembly of the V_1 and V_o subcomplexes (Fig. 1*B*), the assembly state of the complex is commonly assessed by probing for presence of subunits from both V_1 and V_o subcomplexes. Western blot analysis of the fractions eluted from the FLAG column using antibodies against both *a*4-FLAG (V_o) and the catalytic A subunit (V_1) revealed the presence of intact V-ATPase (Fig. 2*B*). The peak fractions were then concentrated and applied to a glycerol density gradient, which revealed two overlapping peaks, one containing isolated V_o, and the other, intact holo V-ATPase (Fig. 2*C*). Silver-stained SDS-PAGE of gradient fractions confirms the presence of all major enzyme subunits for V-ATPase and V_o complexes (Fig. 2*D*). The average yield from 20 g of cells (~1.6 l culture) of purified, nanodisc-reconstituted V_o and intact V-ATPase is ~100 μg and
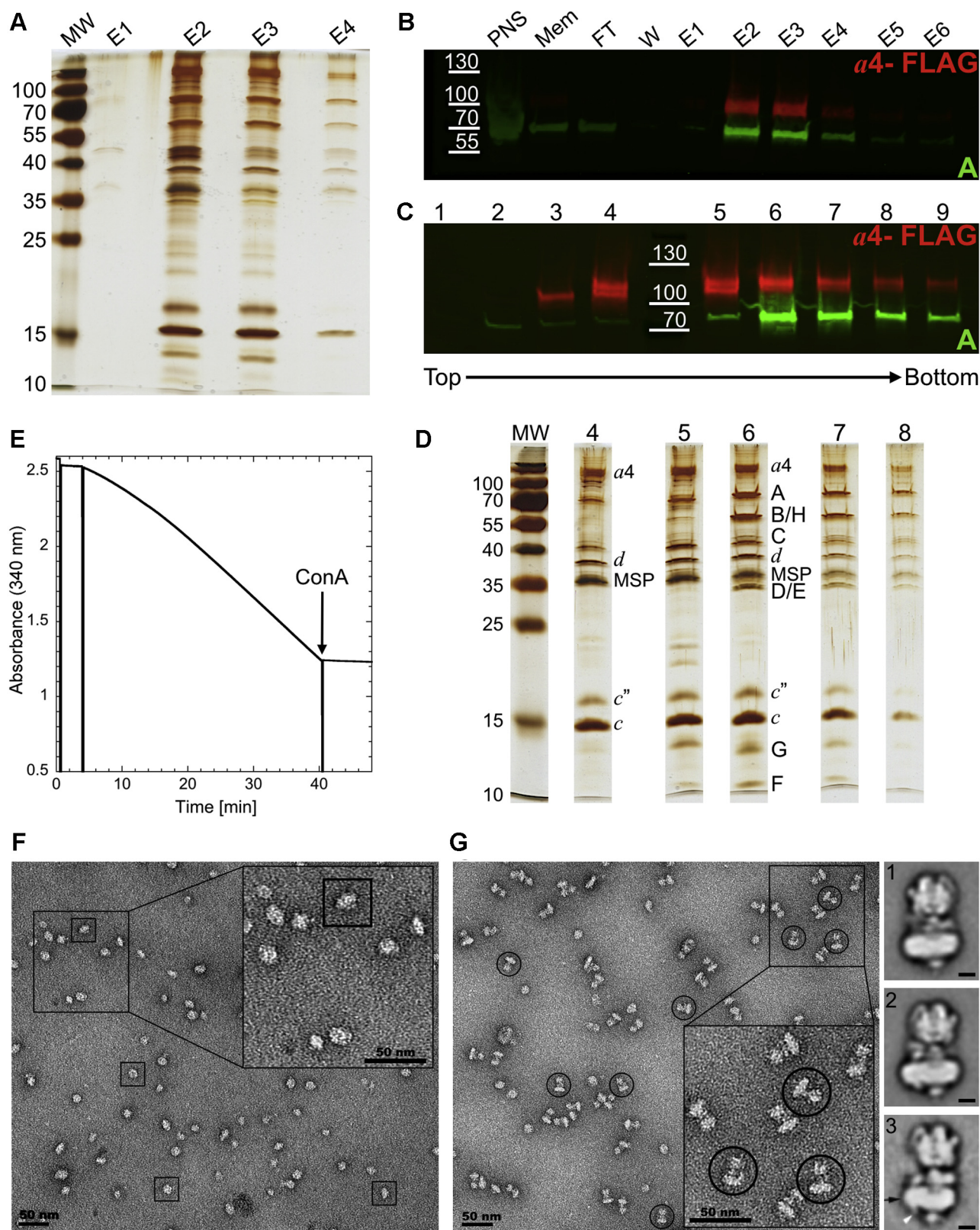
Figure 2. Purification of the human *a*4-containing V-ATPase. *A*, silver-stained SDS-PAGE showing peak FLAG elution fractions (E1-E4). *B*, Western blot analysis of purification steps (probed for FLAG tag on *a*4 (*red*) and catalytic A subunit, ATP6V1A (*green*)). *C*, Western blot of density gradient fractions probed as in panel *B*. *D*, silver-stained SDS-PAGE of peak gradient fractions. *E*, ATPase assay with 1.3-μg purified V-ATPase. At the indicated time, 200 nM ConA was added to the assay. *F* and *G*, negative-stain electron microscopy of purified V_o (*F*) and holo V-ATPase (*G*). Class averages (images 1 and 2) of intact V-ATPase are shown next to panel *G*. For comparison, image 3 shows a two-dimensional average of bovine brain V-ATPase (59). Bar in class averages 1 to 3 is 5 nm. Selections of intact V-ATPases and V_o complexes are highlighted by *circles* and *squares*, respectively. E1-E6, FLAG elution fractions; FT, unbound material from the FLAG column; MEM, membrane fraction; PNS, cell lysate after removal of unbroken cells and nuclei; V-ATPase, vacuolar H^+-ATPase; V_o, membrane integral proton channel; W, column wash.

135 µg, respectively. Moreover, fractions containing the intact enzyme display a specific activity of ~2 to 5 µmol × (min × mg)$^{-1}$ (3.7 ± 0.9 (s.e.m) µmol × (min × mg)$^{-1}$ for three independent preparations) that is inhibited >95% by the specific V-ATPase inhibitor ConA (Fig. 2E). ConA inhibits V-ATPase by binding to the *c*-ring in V$_o$; therefore, ATP hydrolysis (on V$_1$) that is inhibited by ConA indicates that the enzyme is properly assembled and functionally coupled (82, 86). Analysis of the gradient fractions containing isolated V$_o$ and intact V-ATPase (Fig. 2, F and G) by negative-stain electron microscopy reveals that the samples are monodisperse with the characteristic morphology for the two complexes.

In humans, although a core set of subunits are invariant (A, D, F, *f* and *c*-ring), many subunits (B, C, E, G, H, *a*, *d*, *e*) are expressed as multiple isoforms or as splice variants with some tissue enriched and others ubiquitously expressed (44, 45). As expression of isoform *a*4 is enriched in the kidney along with V$_1$ subunit isoforms B1, C2, E1, and G3 and V$_o$ isoform *d*2 (5, 87, 88), it was of interest to analyze which subunit isoforms co-purified with exogenously expressed *a*4. MS analysis revealed the presence of largely ubiquitous subunit isoforms (B2, C1, E1, G1, and *d*1) copurifying with isoform *a*4 (Fig. 3, A and B, Figs. S3–S5, Supplemental Data 1). However, lower scoring hits included tissue-specific isoforms (B1, C2 (kidney), E2 (testes), G2 (brain)) (44, 87–89) and may indicate the presence of minor populations or "hybrid" complexes containing multiple isoforms of multicopy subunits, as had been suggested previously for V-ATPase immunoprecipitated from murine kidney (66). Our analysis indicates that when exogenously expressed in HEK cells, *a*4 forms a fully functional complex containing isoforms B2, C1, G1, E1, and *d*1, likely to be the more abundant ones present in these cells. Therefore, this purified complex differs from the major kidney V-ATPase in V$_1$ subunit isoforms B, C, and G. Interestingly, it was previously found that despite the enrichment of *d*2 expression in

the kidney, isoform *d*1 is part of the renal V-ATPase (66) and as such the composition (*a*4, *d*1) of the V$_o$ complex presented here contains the same isoform composition as that found enriched in renal cells. While containing some differences in the isoform content, the specific activity of the purified complex presented here is similar to that previously reported for bovine kidney V-ATPase (73).

MS analysis of gradient fractions also revealed the presence of factors required for biosynthetic assembly of the V$_o$ complex (Fig. 3, A and B and Figs. S3–S5, Supplemental Data 1), with the denser of the two peak V$_o$-containing fractions enriched in assembly factors (Fig. S6). Biosynthetic assembly of the V$_o$ complex occurs in the endoplasmic reticulum, and although well characterized in yeast (90), less is known about the process in mammals. Recently, mammalian orthologs to yeast assembly factors Vma22p, Vma12p, and Vma21p (91–93) have been identified as coiled-coil domain–containing protein 115, transmembrane protein 199, and vacuolar H$^+$-ATPase assembly integral membrane protein 21, respectively (94–96). Our analysis indicates that along with intact V-ATPase, and V$_o$, purification from organelle membranes using tagged isoform *a*4 permitted isolation of assembly intermediates from the endoplasmic reticulum membrane. Furthermore, overexpression of *a*4 may lead to some saturation of the assembly pathway, permitting capture of what would otherwise be transient assembly intermediates and providing exciting new opportunities for the study of enzyme assembly in humans.

Discussion

Here, we report purification of lipid nanodisc reconstituted human V-ATPase with defined *a* subunit isoform composition. Stably expressed isoform *a*4 associates with ubiquitous isoforms of other enzyme subunits to form an active complex. The preparation is monodisperse and displays robust specific
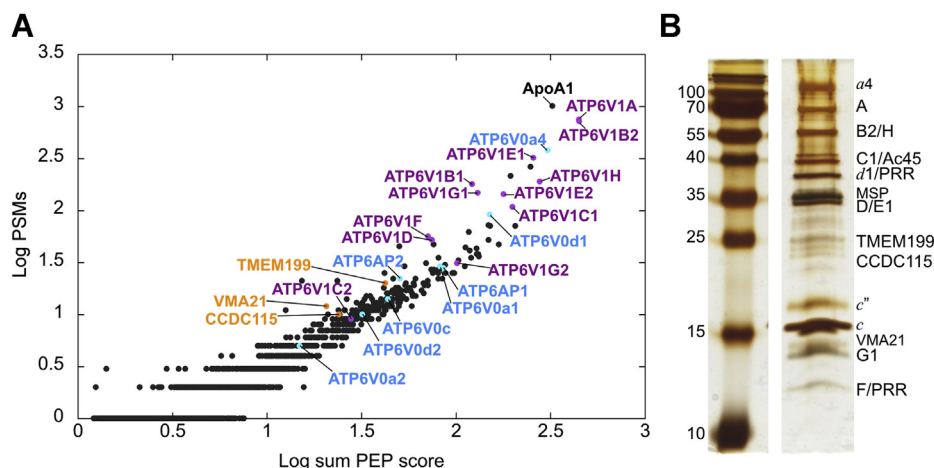

Figure 3. MS analysis of the purified *a*4-containing human V-ATPase. *A*, plot showing proteins identified by MS in gradient fraction 6 (see Fig. 2, C and D), labeled with gene names of V-ATPase subunits and accessory proteins (V$_1$, *purple*; V$_o$, *blue*), as well as assembly factors (*orange*). ApoA1 corresponds to the membrane scaffold protein (MSP) from the lipid nanodiscs. PEP score = sum of the negative log of PEP values for associated PSMs (Proteome Discoverer). *B*, silver-stained SDS-PAGE gel labeled with subunit isoforms, accessory proteins, and assembly factors identified by MS analysis of excised bands (Figs. S4 and S5). The *c*-ring subunits (*c*, *c''*) were annotated based on their characteristic staining patterns. PEP, posterior error probability; PSMs, peptide spectrum matches; V-ATPase, vacuolar H$^+$-ATPase; V$_o$, membrane integral proton channel; V$_1$, cytosolic ATPase subcomplex.

activity that is >95% ConA sensitive. The yield of purified holo V-ATPase is ~85 μg per liter of culture, approximately eight times higher than that reported for affinity capture of endogenous human enzyme using SidK (97), highlighting the utility and efficiency of moderate and stable overexpression of isoforms for purification. Our procedure provides a means for purification of active human V-ATPase that is suitable for biochemical and structural studies. Next to holo V-ATPase, the protocol also allowed purification of isolated V_o complexes. Free autoinhibited V_o, which can be generated as a result of V-ATPase regulation by reversible disassembly *in vivo*, is stabilized by a conformational change in subunit *a* (25, 98). In yeast, enzymes containing different *a* isoforms have different propensities to undergo this mode of regulation (48, 51). In mammals, V-ATPases containing isoform *a*1 (enriched in the brain) reversibly disassemble (37), and autoinhibited V_o has been purified and characterized from bovine brain clathrin-coated vesicles (27, 98). However, it remains unclear whether reversible disassembly in mammals is restricted to specific isoforms, as in yeast. Previously, we have presented a defined *in vitro* system for analysis of reversible disassembly of the yeast V-ATPase using purified V_1 and V_o subcomplexes (99). Establishment of such a system for the human enzyme will benefit from purified human V_o subcomplexes of defined isoform composition. Such studies will further our understanding about this mode of regulation in humans, information that will be required as reversible disassembly has been proposed as a possible target for therapeutic modulation of enzyme function (100). Furthermore, although much recent progress has been made on the structure of the mammalian enzyme (22, 24), including from humans (23), there is currently no high-resolution information for the isolated V_o complex from mammals. Moreover, we have isolated a population of V_o bound to assembly factors, likely constituting assembly intermediates. Mutations in assembly factors coiled-coil domain–containing protein 115, transmembrane protein 199, and vacuolar ATPase assembly integral membrane protein 21 (VMA21) cause abnormal protein glycosylation disorders and liver disease (94, 95, 101), and as such, a more thorough characterization of the assembly process in mammals is needed. The purification of such complexes will provide a valuable tool for furthering our understanding of the V-ATPase assembly process in humans.

Taken together, the approach presented here provides a new tool and a platform for addressing questions related to enzyme function, biochemical properties, regulation, and biosynthetic assembly, in an isoform-specific way. This strategy can, in principle, be extended to expression of other *a* isoforms, thereby shedding light on whether various isoform-containing V-ATPases display inherently different specific biochemical properties as observed in yeast. Purified, active human V-ATPase will simplify the analysis of potential V-ATPase regulators and binding partners, allowing examination of their direct effects on enzyme activity and/or assembly. Importantly, as specific *a* isoforms are upregulated and mislocalized in cancer cells, purified, active human enzyme of defined *a* isoform composition will have the potential to greatly assist in the

selection, development, and characterization of isoform-targeted therapeutics.

Experimental procedures

A detailed description of human cell culture and biochemical experiments and a table containing information for key resources can be found in SI Methods.

Expression and purification of MSP

MSP1E3D1 carrying N-terminal 7× His and Avi tags separated by a PreScission protease cleavage site was expressed and purified as previously described (99), with modifications detailed in SI Methods. Briefly, MSP was expressed in *Escherichia coli* BL21(DE3) and purified using Ni-NTA affinity chromatography. MSP was dialyzed against low-ionic strength buffer, lyophilized, and stored at –80 °C until use.

Isoform a4-2× -FLAG stable expression and cell growth

Suspension HEK cells (293F; FreeStyle cells) were maintained in FreeStyle media in vented shake flasks at 37 °C in a humidified 8% CO_2 atmosphere. Cells were transfected with a pcDNA3.1 vector containing the coding sequence for isoform *a*4 (ATP6V0a4) carrying a C-terminal 2× FLAG tag (78) and selected for using Geneticin. For protein purification, 1.6-l batches of cells were harvested by centrifugation, flash-frozen in liquid nitrogen, and stored at –80 °C until use.

Purification of human V-ATPase in lipid nanodiscs

A detailed method for purification of the human V-ATPase can be found in SI Methods. Briefly, cells (~20 g) were lysed in a Dounce homogenizer, and unbroken cells and nuclei were removed by low-speed centrifugation. A dense membrane/organelle fraction was collected by centrifugation (14,600g), resuspended at ~16 mg/ml membrane protein in ~15 mg/ml MSP, and extracted in 1% dodecyl maltoside. After detergent removal with 0.4 g/ml Bio-Beads, nanodisc-reconstituted membrane protein was mixed with 1.5 ml of αFLAG resin for affinity capture of FLAG-tagged *a*4-containing complexes. Elution fractions were pooled, concentrated, and applied to an 11-ml (20–50%) glycerol density gradient. Fractions were collected from the top of the gradient and analyzed by Western blot and silver-stain SDS-PAGE, and protein concentration was determined using a modified Pierce BCA assay.

Immunoblot

Samples were separated on gradient SDS-PAGE (4–20% acrylamide) gels, transferred to low-fluorescence polyvinylidene difluoride membranes, and probed for the catalytic A subunit (ATP6V1A) and the FLAG tag on *a*4. Details can be found in SI Methods. Antibody source information is listed in the Key Resources Table.

ATPase activity measurements

ConA-sensitive ATPase activities were measured at 37 °C using a coupled enzyme assay as previously described (29, 99).

Negative-stain electron microscopy

Samples were spotted on carbon-coated copper grids and stained with 1% uranyl acetate. Grids were examined in a JEM-1400 transmission electron microscope (JEOL) operating at 80 kV. Micrographs were recorded with an Orius SC1000 (model 832) CCD camera (Gatan Inc) at 200,000× magnification. Two-dimensional averages were generated as described in SI Methods. Briefly, a dataset of ~15,400 particles selected from 40 micrographs was processed as described (75).

MS sample preparation and analyses

In-gel trypsin digestion was carried out on excised gel bands from two independent purifications. In-solution digestion of peak gradient fractions was carried out using filter-assisted sample preparation (102) and peptides desalted using mixed-mode cation exchange stage tips (103). For LC-MS/MS, samples were dissolved in water containing 2% acetonitrile and 0.5% formic acid. Samples (0.5 μg) were injected onto a nano-LC (C18) column connected inline to an Orbitrap Lumos mass spectrometer *via* a nanoelectrospray source operating at 2.2 kV. The MS data were searched using Sequest HT in Proteome Discoverer (version 2.4, Thermo Scientific) against the human proteome in UniProt. Label-free quantification was performed in Proteome Discoverer. Details of the MS sample preparation and analyses can be found in SI Methods.

Data availability

All data presented are contained within the article and supporting information. Raw MS data were deposited into the Figshare data repository under 10.6084/m9.figshare.14589453.

Abbreviations—The abbreviations used are: ConA, concanamycin A; MSP, membrane scaffold protein; V-ATPase, vacuolar H$^+$-ATPase; V$_o$, membrane integral proton transport subcomplex; V$_1$, cytosolic ATPase subcomplex; VMA21, vacuolar ATPase assembly integral membrane protein 21.

References

1. Collins, M. P., and Forgac, M. (2020) Regulation and function of V-ATPases in physiology and disease. *Biochim. Biophys. Acta Biomembr.* **1862**, 183341
2. Eaton, A. F., Merkulova, M., and Brown, D. (2021) The H(+)-ATPase (V-ATPase): From proton pump to signaling complex in health and disease. *Am. J. Physiol. Cell Physiol.* **320**, C392–C414
3. Blair, H. C., Teitelbaum, S. L., Ghiselli, R., and Gluck, S. (1989) Osteoclastic bone resorption by a polarized vacuolar proton pump. *Science* **245**, 855–857
4. Wagner, C. A., Finberg, K. E., Breton, S., Marshansky, V., Brown, D., and Geibel, J. P. (2004) Renal vacuolar H+-ATPase. *Physiol. Rev.* **84**, 1263–1314
5. Smith, A. N., Skaug, J., Choate, K. A., Nayir, A., Bakkaloglu, A., Ozen, S., Hulton, S. A., Sanjad, S. A., Al-Sabban, E. A., Lifton, R. P., Scherer, S. W., and Karet, F. E. (2000) Mutations in ATP6N1B, encoding a new kidney vacuolar proton pump 116-kD subunit, cause recessive distal renal tubular acidosis with preserved hearing. *Nat. Genet.* **26**, 71–75
6. Frattini, A., Orchard, P. J., Sobacchi, C., Giliani, S., Abinun, M., Mattsson, J. P., Keeling, D. J., Andersson, A. K., Wallbrandt, P., Zecca, L., Notarangelo, L. D., Vezzoni, P., and Villa, A. (2000) Defects in TCIRG1 subunit of the vacuolar proton pump are responsible for a subset of human autosomal recessive osteopetrosis. *Nat. Genet.* **25**, 343–346
7. Colacurcio, D. J., and Nixon, R. A. (2016) Disorders of lysosomal acidification-the emerging role of V-ATPase in aging and neurodegenerative disease. *Ageing Res. Rev.* **32**, 75–88
8. Bagh, M. B., Peng, S., Chandra, G., Zhang, Z., Singh, S. P., Pattabiraman, N., Liu, A., and Mukherjee, A. B. (2017) Misrouting of V-ATPase subunit V0a1 dysregulates lysosomal acidification in a neurodegenerative lysosomal storage disease model. *Nat. Commun.* **8**, 14612
9. Hucthagowder, V., Morava, E., Kornak, U., Lefeber, D. J., Fischer, B., Dimopoulou, A., Aldinger, A., Choi, J., Davis, E. C., Abuelo, D. N., Adamowicz, M., Al-Aama, J., Basel-Vanagaite, L., Fernandez, B., Greally, M. T., *et al.* (2009) Loss-of-function mutations in ATP6V0A2 impair vesicular trafficking, tropoelastin secretion and cell survival. *Hum. Mol. Genet.* **18**, 2149–2165
10. Stransky, L., Cotter, K., and Forgac, M. (2016) The function of V-ATPases in cancer. *Physiol. Rev.* **96**, 1071–1091
11. Xu, L., Shen, X., Bryan, A., Banga, S., Swanson, M. S., and Luo, Z. Q. (2010) Inhibition of host vacuolar H+-ATPase activity by a Legionella pneumophila effector. *PLoS Pathog.* **6**, e1000822
12. Wong, D., Bach, H., Sun, J., Hmama, Z., and Av-Gay, Y. (2011) Mycobacterium tuberculosis protein tyrosine phosphatase (PtpA) excludes host vacuolar-H+-ATPase to inhibit phagosome acidification. *Proc. Natl. Acad. Sci. U. S. A.* **108**, 19371–19376
13. Sreelatha, A., Bennett, T. L., Carpinone, E. M., O'Brien, K. M., Jordan, K. D., Burdette, D. L., Orth, K., and Starai, V. J. (2015) Vibrio effector protein VopQ inhibits fusion of V-ATPase-containing membranes. *Proc. Natl. Acad. Sci. U. S. A.* **112**, 100–105
14. Lu, X., Yu, H., Liu, S. H., Brodsky, F. M., and Peterlin, B. M. (1998) Interactions between HIV1 Nef and vacuolar ATPase facilitate the internalization of CD4. *Immunity* **8**, 647–656
15. Marjuki, H., Gornitzky, A., Marathe, B. M., Ilyushina, N. A., Aldridge, J. R., Desai, G., Webby, R. J., and Webster, R. G. (2011) Influenza A virus-induced early activation of ERK and PI3K mediates V-ATPase-dependent intracellular pH change required for fusion. *Cell. Microbiol.* **13**, 587–601
16. Lindstrom, A., Anantpadma, M., Baker, L., Raghavendra, N. M., Davey, R., and Davisson, V. J. (2018) Phenotypic prioritization of diphyllin derivatives that block filo-viral cell entry by vacuolar (H+)-ATPase inhibition. *ChemMedChem* **13**, 2664–2676

ASBMB

J. Biol. Chem. (2021) 297(2) 100964 **7**

17. Perreira, J. M., Aker, A. M., Savidis, G., Chin, C. R., McDougall, W. M., Portmann, J. M., Meraner, P., Smith, M. C., Rahman, M., Baker, R. E., Gauthier, A., Franti, M., and Brass, A. L. (2015) RNASEK is a V-ATPase-associated factor required for endocytosis and the replication of rhinovirus, influenza A virus, and dengue virus. *Cell Rep.* **12**, 850–863

18. Gordon, D. E., Jang, G. M., Bouhaddou, M., Xu, J., Obernier, K., White, K. M., O'Meara, M. J., Rezelj, V. V., Guo, J. Z., Swaney, D. L., Tummino, T. A., Hüttenhain, R., Kaake, R. M., Richards, A. L., Tutuncuoglu, B., *et al.* (2020) A SARS-CoV-2 protein interaction map reveals targets for drug repurposing. *Nature* **583**, 459–468

19. Vasanthakumar, T., and Rubinstein, J. L. (2020) Structure and roles of V-type ATPases. *Trends Biochem. Sci.* **45**, 295–307

20. Supek, F., Supekova, L., Mandiyan, S., Pan, Y. C., Nelson, H., and Nelson, N. (1994) A novel accessory subunit for vacuolar H(+)-ATPase from chromaffin granules. *J. Biol. Chem.* **269**, 24102–24106

21. Ludwig, J., Kerscher, S., Brandt, U., Pfeiffer, K., Getlawi, F., Apps, D. K., and Schägger, H. (1998) Identification and characterization of a novel 9. 2-kDa membrane sector-associated protein of vacuolar proton-ATPase from chromaffin granules. *J. Biol. Chem.* **273**, 10939–10947

22. Abbas, Y. M., Wu, D., Bueler, S. A., Robinson, C. V., and Rubinstein, J. L. (2020) Structure of V-ATPase from the mammalian brain. *Science* **367**, 1240–1246

23. Wang, L., Wu, D., Robinson, C. V., Wu, H., and Fu, T. M. (2020) Structures of a complete human V-ATPase reveal mechanisms of its assembly. *Mol. Cell* **80**, 501–511.e503

24. Wang, R., Long, T., Hassan, A., Wang, J., Sun, Y., Xie, X. S., and Li, X. (2020) Cryo-EM structures of intact V-ATPase from bovine brain. *Nat. Commun.* **11**, 3921

25. Roh, S. H., Shekhar, M., Pintilie, G., Chipot, C., Wilkens, S., Singharoy, A., and Chiu, W. (2020) Cryo-EM and MD infer water-mediated proton transport and autoinhibition mechanisms of Vo complex. *Sci. Adv.* **6**, eabb9605

26. Oot, R. A., Couoh-Cardel, S., Sharma, S., Stam, N. J., and Wilkens, S. (2017) Breaking up and making up: The secret life of the vacuolar H(+)-ATPase. *Protein Sci.* **26**, 896–909

27. Zhang, J., Myers, M., and Forgac, M. (1992) Characterization of the V0 domain of the coated vesicle (H+)-ATPase. *J. Biol. Chem.* **267**, 9773–9778

28. Parra, K. J., Keenan, K. L., and Kane, P. M. (2000) The H subunit (Vma13p) of the yeast V-ATPase inhibits the ATPase activity of cytosolic V1 complexes. *J. Biol. Chem.* **275**, 21761–21767

29. Zhang, Z., Charsky, C., Kane, P. M., and Wilkens, S. (2003) Yeast V1-ATPase: Affinity purification and structural features by electron microscopy. *J. Biol. Chem.* **278**, 47299–47306

30. Couoh-Cardel, S., Milgrom, E., and Wilkens, S. (2015) Affinity purification and structural features of the yeast vacuolar ATPase Vo membrane sector. *J. Biol. Chem.* **290**, 27959–27971

31. Kane, P. M. (1995) Disassembly and reassembly of the yeast vacuolar H(+)-ATPase *in vivo*. *J. Biol. Chem.* **270**, 17025–17032

32. Parra, K. J., and Kane, P. M. (1998) Reversible association between the V1 and V0 domains of yeast vacuolar H+-ATPase is an unconventional glucose-induced effect. *Mol. Cell. Biol.* **18**, 7064–7074

33. Sumner, J. P., Dow, J. A., Earley, F. G., Klein, U., Jager, D., and Wieczorek, H. (1995) Regulation of plasma membrane V-ATPase activity by dissociation of peripheral subunits. *J. Biol. Chem.* **270**, 5649–5653

34. Graf, R., Harvey, W. R., and Wieczorek, H. (1996) Purification and properties of a cytosolic V1-ATPase. *J. Biol. Chem.* **271**, 20908–20913

35. Trombetta, E. S., Ebersold, M., Garrett, W., Pypaert, M., and Mellman, I. (2003) Activation of lysosomal function during dendritic cell maturation. *Science* **299**, 1400–1403

36. Liberman, R., Bond, S., Shainheit, M. G., Stadecker, M. J., and Forgac, M. (2014) Regulated assembly of vacuolar ATPase is increased during cluster disruption-induced maturation of dendritic cells through a phosphatidylinositol 3-kinase/mTOR-dependent pathway. *J. Biol. Chem.* **289**, 1355–1363

37. Bodzeta, A., Kahms, M., and Klingauf, J. (2017) The presynaptic V-ATPase reversibly disassembles and thereby modulates exocytosis but is not part of the fusion machinery. *Cell Rep.* **20**, 1348–1359

38. Xu, Y., Parmar, A., Roux, E., Balbis, A., Dumas, V., Chevalier, S., and Posner, B. I. (2012) Epidermal growth factor-induced vacuolar (H+)-atpase assembly: A role in signaling via mTORC1 activation. *J. Biol. Chem.* **287**, 26409–26422

39. Lafourcade, C., Sobo, K., Kieffer-Jaquinod, S., Garin, J., and van der Goot, F. G. (2008) Regulation of the V-ATPase along the endocytic pathway occurs through reversible subunit association and membrane localization. *PLoS One* **3**, e2758

40. Dechant, R., Binda, M., Lee, S. S., Pelet, S., Winderickx, J., and Peter, M. (2010) Cytosolic pH is a second messenger for glucose and regulates the PKA pathway through V-ATPase. *EMBO J.* **29**, 2515–2526

41. Sautin, Y. Y., Lu, M., Gaugler, A., Zhang, L., and Gluck, S. L. (2005) Phosphatidylinositol 3-kinase-mediated effects of glucose on vacuolar H+-ATPase assembly, translocation, and acidification of intracellular compartments in renal epithelial cells. *Mol. Cell. Biol.* **25**, 575–589

42. McGuire, C. M., and Forgac, M. (2018) Glucose starvation increases V-ATPase assembly and activity in mammalian cells through AMP kinase and phosphatidylinositide 3-kinase/Akt signaling. *J. Biol. Chem.* **293**, 9113–9123

43. Collins, M. P., Stransky, L. A., and Forgac, M. (2020) AKT Ser/Thr kinase increases V-ATPase-dependent lysosomal acidification in response to amino acid starvation in mammalian cells. *J. Biol. Chem.* **295**, 9433–9444

44. Toei, M., Saum, R., and Forgac, M. (2010) Regulation and isoform function of the V-ATPases. *Biochemistry* **49**, 4715–4723

45. Futai, M., Sun-Wada, G. H., Wada, Y., Matsumoto, N., and Nakanishi-Matsui, M. (2019) Vacuolar-type ATPase: A proton pump to lysosomal trafficking. *Proc. Jpn. Acad. Ser. B Phys. Biol. Sci.* **95**, 261–277

46. Manolson, M. F., Proteau, D., Preston, R. A., Stenbit, A., Roberts, B. T., Hoyt, M. A., Preuss, D., Mulholland, J., Botstein, D., and Jones, E. W. (1992) The VPH1 gene encodes a 95-kDa integral membrane polypeptide required for in vivo assembly and activity of the yeast vacuolar H(+)-ATPase. *J. Biol. Chem.* **267**, 14294–14303

47. Manolson, M. F., Wu, B., Proteau, D., Taillon, B. E., Roberts, B. T., Hoyt, M. A., and Jones, E. W. (1994) STV1 gene encodes functional homologue of 95-kDa yeast vacuolar H(+)-ATPase subunit Vph1p. *J. Biol. Chem.* **269**, 14064–14074

48. Kawasaki-Nishi, S., Bowers, K., Nishi, T., Forgac, M., and Stevens, T. H. (2001) The amino-terminal domain of the vacuolar proton-translocating ATPase a subunit controls targeting and *in vivo* dissociation, and the carboxyl-terminal domain affects coupling of proton transport and ATP hydrolysis. *J. Biol. Chem.* **276**, 47411–47420

49. Kawasaki-Nishi, S., Nishi, T., and Forgac, M. (2001) Yeast V-ATPase complexes containing different isoforms of the 100-kDa a-subunit differ in coupling efficiency and *in vivo* dissociation. *J. Biol. Chem.* **276**, 17941–17948

50. Finnigan, G. C., Cronan, G. E., Park, H. J., Srinivasan, S., Quiocho, F. A., and Stevens, T. H. (2012) Sorting of the yeast vacuolar-type, proton-translocating ATPase enzyme complex (V-ATPase): Identification of a necessary and sufficient Golgi/endosomal retention signal in Stv1p. *J. Biol. Chem.* **287**, 19487–19500

51. Smardon, A. M., Diab, H. I., Tarsio, M., Diakov, T. T., Nasab, N. D., West, R. W., and Kane, P. M. (2014) The RAVE complex is an isoform-specific V-ATPase assembly factor in yeast. *Mol. Biol. Cell* **25**, 356–367

52. Vasanthakumar, T., Bueler, S. A., Wu, D., Beilsten-Edmands, V., Robinson, C. V., and Rubinstein, J. L. (2019) Structural comparison of the vacuolar and Golgi V-ATPases from Saccharomyces cerevisiae. *Proc. Natl. Acad. Sci. U. S. A.* **116**, 7272–7277

53. Morel, N., Dedieu, J. C., and Philippe, J. M. (2003) Specific sorting of the a1 isoform of the V-H+ATPase a subunit to nerve terminals where it associates with both synaptic vesicles and the presynaptic plasma membrane. *J. Cell Sci.* **116**, 4751–4762

54. Vavassori, S., and Mayer, A. (2014) A new life for an old pump: V-ATPase and neurotransmitter release. *J. Cell Biol.* **205**, 7–9

55. Fischer, B., Dimopoulou, A., Egerer, J., Gardeitchik, T., Kidd, A., Jost, D., Kayserili, H., Alanay, Y., Tantcheva-Poor, I., Mangold, E., Daumer-Haas, C., Phadke, S., Peirano, R. I., Heusel, J., *et al.* (2012) Further

≋ASBMB

characterization of ATP6V0A2-related autosomal recessive cutis laxa. *Hum. Genet.* **131**, 1761–1773

56. Hurtado-Lorenzo, A., Skinner, M., El Annan, J., Futai, M., Sun-Wada, G. H., Bourgoin, S., Casanova, J., Wildeman, A., Bechoua, S., Ausiello, D. A., Brown, D., and Marshansky, V. (2006) V-ATPase interacts with ARNO and Arf6 in early endosomes and regulates the protein degradative pathway. *Nat. Cell Biol.* **8**, 124–136

57. Toyomura, T., Murata, Y., Yamamoto, A., Oka, T., Sun-Wada, G. H., Wada, Y., and Futai, M. (2003) From lysosomes to the plasma membrane: Localization of vacuolar-type H+ -ATPase with the a3 isoform during osteoclast differentiation. *J. Biol. Chem.* **278**, 22023–22030

58. Chitirala, P., Ravichandran, K., Schirra, C., Chang, H. F., Krause, E., Kazmaier, U., Lauterbach, M. A., and Rettig, J. (2020) Role of V-ATPase a3-subunit in mouse CTL function. *J. Immunol.* **204**, 2818–2828

59. Sun-Wada, G. H., Toyomura, T., Murata, Y., Yamamoto, A., Futai, M., and Wada, Y. (2006) The a3 isoform of V-ATPase regulates insulin secretion from pancreatic beta-cells. *J. Cell Sci.* **119**, 4531–4540

60. Lorente-Canovas, B., Ingham, N., Norgett, E. E., Golder, Z. J., Karet Frankl, F. E., and Steel, K. P. (2013) Mice deficient in H+-ATPase a4 subunit have severe hearing impairment associated with enlarged endolymphatic compartments within the inner ear. *Dis. Model Mech.* **6**, 434–442

61. Norgett, E. E., Golder, Z. J., Lorente-Canovas, B., Ingham, N., Steel, K. P., and Karet Frankl, F. E. (2012) Atp6v0a4 knockout mouse is a model of distal renal tubular acidosis with hearing loss, with additional extrarenal phenotype. *Proc. Natl. Acad. Sci. U. S. A.* **109**, 13775–13780

62. Smith, A. N., Finberg, K. E., Wagner, C. A., Lifton, R. P., Devonald, M. A., Su, Y., and Karet, F. E. (2001) Molecular cloning and characterization of Atp6n1b: A novel fourth murine vacuolar H+-ATPase a-subunit gene. *J. Biol. Chem.* **276**, 42382–42388

63. Pietrement, C., Sun-Wada, G. H., Silva, N. D., McKee, M., Marshansky, V., Brown, D., Futai, M., and Breton, S. (2006) Distinct expression patterns of different subunit isoforms of the V-ATPase in the rat epididymis. *Biol. Reprod.* **74**, 185–194

64. Matsumoto, N., Daido, S., Sun-Wada, G. H., Wada, Y., Futai, M., and Nakanishi-Matsui, M. (2014) Diversity of proton pumps in osteoclasts: V-ATPase with A3 and D2 isoforms is a major form in osteoclasts. *Biochim. Biophys. Acta* **1837**, 744–749

65. Kartner, N., Yao, Y., Li, K., Crasto, G. J., Datti, A., and Manolson, M. F. (2010) Inhibition of osteoclast bone resorption by disrupting vacuolar H+-ATPase A3-B2 subunit interaction. *J. Biol. Chem.* **285**, 37476–37490

66. Merkulova, M., Păunescu, T. G., Azroyan, A., Marshansky, V., Breton, S., and Brown, D. (2015) Mapping the H(+) (V)-ATPase interactome: Identification of proteins involved in trafficking, folding, assembly and phosphorylation. *Sci. Rep.* **5**, 14827

67. Aoto, K., Kato, M., Akita, T., Nakashima, M., Mutoh, H., Akasaka, N., Tohyama, J., Nomura, Y., Hoshino, K., Ago, Y., Tanaka, R., Epstein, O., Ben-Haim, R., Heyman, E., Miyazaki, T., *et al*. (2021) ATP6V0A1 encoding the a1-subunit of the V0 domain of vacuolar H(+)-ATPases is essential for brain development in humans and mice. *Nat. Commun.* **12**, 2107

68. Kornak, U., Reynders, E., Dimopoulou, A., van Reeuwijk, J., Fischer, B., Rajab, A., Budde, B., Nürnberg, P., Foulquier, F., ARCL Debré-type Study Group, Lefeber, D., Urban, Z., Gruenewald, S., Annaert, W., Brunner, H. G., *et al*. (2008) Impaired glycosylation and cutis laxa caused by mutations in the vesicular H+-ATPase subunit ATP6V0A2. *Nat. Genet.* **40**, 32–34

69. Cotter, K., Liberman, R., Sun-Wada, G., Wada, Y., Sgroi, D., Naber, S., Brown, D., Breton, S., and Forgac, M. (2016) The a3 isoform of subunit a of the vacuolar ATPase localizes to the plasma membrane of invasive breast tumor cells and is overexpressed in human breast cancer. *Oncotarget* **7**, 46142–46157

70. Inoue, H., Noumi, T., Nagata, M., Murakami, H., and Kanazawa, H. (1999) Targeted disruption of the gene encoding the proteolipid subunit of mouse vacuolar H(+)-ATPase leads to early embryonic lethality. *Biochim. Biophys. Acta* **1413**, 130–138

71. Sun-Wada, G., Murata, Y., Yamamoto, A., Kanazawa, H., Wada, Y., and Futai, M. (2000) Acidic endomembrane organelles are required for mouse postimplantation development. *Dev. Biol.* **228**, 315–325

72. Arai, H., Berne, M., Terres, G., Terres, H., Puopolo, K., and Forgac, M. (1987) Subunit composition and ATP site labeling of the coated vesicle proton-translocating adenosinetriphosphatase. *Biochemistry* **26**, 6632–6638

73. Gluck, S., and Caldwell, J. (1987) Immunoaffinity purification and characterization of vacuolar H+ATPase from bovine kidney. *J. Biol. Chem.* **262**, 15780–15789

74. Mattsson, J. P., Schlesinger, P. H., Keeling, D. J., Teitelbaum, S. L., Stone, D. K., and Xie, X. S. (1994) Isolation and reconstitution of a vacuolar-type proton pump of osteoclast membranes. *J. Biol. Chem.* **269**, 24979–24982

75. Wilkens, S., Vasilyeva, E., and Forgac, M. (1999) Structure of the vacuolar ATPase by electron microscopy. *J. Biol. Chem.* **274**, 31804–31810

76. Nelson, N. (2003) A journey from mammals to yeast with vacuolar H+-ATPase (V-ATPase). *J. Bioenerg. Biomembr.* **35**, 281–289

77. Muench, S. P., Huss, M., Song, C. F., Phillips, C., Wieczorek, H., Trinick, J., and Harrison, M. A. (2009) Cryo-electron microscopy of the vacuolar ATPase motor reveals its mechanical and regulatory complexity. *J. Mol. Biol.* **386**, 989–999

78. Esmail, S., Yao, Y., Kartner, N., Li, J., Reithmeier, R. A., and Manolson, M. F. (2016) N-linked glycosylation is required for vacuolar H(+)-ATPase (V-ATPase) a4 subunit stability, assembly, and cell surface expression. *J. Cell. Biochem.* **117**, 2757–2768

79. Esmail, S., Kartner, N., Yao, Y., Kim, J. W., Reithmeier, R. A. F., and Manolson, M. F. (2018) N-linked glycosylation of a subunit isoforms is critical for vertebrate vacuolar H(+)-ATPase (V-ATPase) biosynthesis. *J. Cell. Biochem.* **119**, 861–875

80. Shaw, G., Morse, S., Ararat, M., and Graham, F. L. (2002) Preferential transformation of human neuronal cells by human adenoviruses and the origin of HEK 293 cells. *FASEB J.* **16**, 869–871

81. Lin, Y. C., Boone, M., Meuris, L., Lemmens, I., Van Roy, N., Soete, A., Reumers, J., Moisse, M., Plaisance, S., Drmanac, R., Chen, J., Speleman, F., Lambrechts, D., Van de Peer, Y., *et al*. (2014) Genome dynamics of the human embryonic kidney 293 lineage in response to cell biology manipulations. *Nat. Commun.* **5**, 4767

82. Crider, B. P., and Xie, X. S. (2003) Characterization of the functional coupling of bovine brain vacuolar-type H(+)-translocating ATPase. Effect of divalent cations, phospholipids, and subunit H (SFD). *J. Biol. Chem.* **278**, 44281–44288

83. Xie, X. S., and Stone, D. K. (1988) Partial resolution and reconstitution of the subunits of the clathrin-coated vesicle proton ATPase responsible for Ca2+-activated ATP hydrolysis. *J. Biol. Chem.* **263**, 9859–9867

84. Civjan, N. R., Bayburt, T. H., Schuler, M. A., and Sligar, S. G. (2003) Direct solubilization of heterologously expressed membrane proteins by incorporation into nanoscale lipid bilayers. *Biotechniques* **35**, 556–560, 562-3

85. Sharma, S., and Wilkens, S. (2017) Biolayer interferometry of lipid nanodisc-reconstituted yeast vacuolar H(+)-ATPase. *Protein Sci.* **26**, 1070–1079

86. Huss, M., Ingenhorst, G., Konig, S., Gassel, M., Drose, S., Zeeck, A., Altendorf, K., and Wieczorek, H. (2002) Concanamycin A, the specific inhibitor of V-ATPases, binds to the V(o) subunit c. *J. Biol. Chem.* **277**, 40544–40548

87. Nelson, R. D., Guo, X. L., Masood, K., Brown, D., Kalkbrenner, M., and Gluck, S. (1992) Selectively amplified expression of an isoform of the vacuolar H(+)-ATPase 56-kilodalton subunit in renal intercalated cells. *Proc. Natl. Acad. Sci. U. S. A.* **89**, 3541–3545

88. Smith, A. N., Borthwick, K. J., and Karet, F. E. (2002) Molecular cloning and characterization of novel tissue-specific isoforms of the human vacuolar H+-ATPase C, G and d subunits, and their evaluation in autosomal recessive distal renal tubular acidosis. *Gene* **297**, 169–177

89. Imai-Senga, Y., Sun-Wada, G. H., Wada, Y., and Futai, M. (2002) A human gene, ATP6E1, encoding a testis-specific isoform of H(+)-ATPase subunit E. *Gene* **289**, 7–12

90. Graham, L. A., Flannery, A. R., and Stevens, T. H. (2003) Structure and assembly of the yeast V-ATPase. *J. Bioenerg. Biomembr.* **35**, 301–312

91. Hill, K. J., and Stevens, T. H. (1994) Vma21p is a yeast membrane protein retained in the endoplasmic reticulum by a di-lysine motif and is required for the assembly of the vacuolar H(+)-ATPase complex. *Mol. Biol. Cell* **5**, 1039–1050

92. Hill, K. J., and Stevens, T. H. (1995) Vma22p is a novel endoplasmic reticulum-associated protein required for assembly of the yeast vacuolar H(+)-ATPase complex. *J. Biol. Chem.* **270**, 22329–22336

93. Jackson, D. D., and Stevens, T. H. (1997) VMA12 encodes a yeast endoplasmic reticulum protein required for vacuolar H+-ATPase assembly. *J. Biol. Chem.* **272**, 25928–25934

94. Jansen, J. C., Cirak, S., van Scherpenzeel, M., Timal, S., Reunert, J., Rust, S., Pérez, B., Vicogne, D., Krawitz, P., Wada, Y., Ashikov, A., Pérez-Cerdá, C., Medrano, C., Arnoldy, A., Hoischen, A., *et al.* (2016) CCDC115 deficiency causes a disorder of Golgi homeostasis with abnormal protein glycosylation. *Am. J. Hum. Genet.* **98**, 310–321

95. Jansen, J. C., Timal, S., van Scherpenzeel, M., Michelakakis, H., Vicogne, D., Ashikov, A., Moraitou, M., Hoischen, A., Huijben, K., Steenbergen, G., van den Boogert, M. A., Porta, F., Calvo, P. L., Mavrikou, M., Cenacchi, G., *et al.* (2016) TMEM199 deficiency is a disorder of Golgi homeostasis characterized by elevated aminotransferases, alkaline phosphatase, and cholesterol and abnormal glycosylation. *Am. J. Hum. Genet.* **98**, 322–330

96. Miles, A. L., Burr, S. P., Grice, G. L., and Nathan, J. A. (2017) The vacuolar-ATPase complex and assembly factors, TMEM199 and CCDC115, control HIF1α prolyl hydroxylation by regulating cellular iron levels. *Elife* **6**, e22693

97. Wang, L., Chen, Z., Wu, H., and Fu, T. M. (2021) Purification and cryoelectron microscopy structure determination of human V-ATPase. *STAR Protoc.* **2**, 100350

98. Wilkens, S., and Forgac, M. (2001) Three-dimensional structure of the vacuolar ATPase proton channel by electron microscopy. *J. Biol. Chem.* **276**, 44064–44068

99. Sharma, S., Oot, R. A., Khan, M. M., and Wilkens, S. (2019) Functional reconstitution of vacuolar H(+)-ATPase from Vo proton channel and mutant V1-ATPase provides insight into the mechanism of reversible disassembly. *J. Biol. Chem.* **294**, 6439–6449

100. Kane, P. M. (2012) Targeting reversible disassembly as a mechanism of controlling V-ATPase activity. *Curr. Protein Pept. Sci.* **13**, 117–123

101. Cannata Serio, M., Graham, L. A., Ashikov, A., Larsen, L. E., Raymond, K., Timal, S., Le Meur, G., Ryan, M., Czarnowska, E., Jansen, J. C., He, M., Ficicioglu, C., Pichurin, P., Hasadsri, L., Ríos-Ocampo, W. A., *et al.* (2020) Mutations in the V-ATPase assembly factor VMA21 cause a congenital disorder of glycosylation with autophagic liver disease. *Hepatology* **72**, 1968–1986

102. Wiśniewski, J. R., Zougman, A., Nagaraj, N., and Mann, M. (2009) Universal sample preparation method for proteome analysis. *Nat. Methods* **6**, 359–362

103. Rappsilber, J., Ishihama, Y., and Mann, M. (2003) Stop and go extraction tips for matrix-assisted laser desorption/ionization, nanoelectrospray, and LC/MS sample pretreatment in proteomics. *Anal. Chem.* **75**, 663–670